Influence of exchange interaction on spin-dependent transport through a single quantum dot doped with a magnetic ion

Fanyao Qu* and P. Vasilopoulos†
Concordia University, Department of Physics, 7141 Sherbrooke Ouest, Montréal, Québec, H3G 1M8, Canada
(Received 30 June 2006; revised manuscript received 17 October 2006; published 8 December 2006)

A quantum theory of single-electron tunneling through a quantum dot (QD), doped with a Mn^{2+} ion and weakly coupled to ferromagnetic (FM) leads in the Coulomb blockade regime, is developed using the sequential tunneling approach and assuming that spin flips do not occur. It predicts a spin-injection-induced magnetization and a spin-dependent current. The spin polarization of the current and the tunneling magnetoresistance (TMR) can be well controlled by a bias voltage and strongly enhanced by the electron-Mn exchange interaction and the spin selectivity of the leads. An appropriate choice of these parameters yields a highly polarized current even when the FM source is not 100% polarized. Analytical expressions for the magnetization, spin-dependent current, spin polarization, and the TMR are derived for zero magnetic field. When the QD is subjected to a strong magnetic field, the numerical calculations predict an oscillatory behavior of the TMR as a function of the bias voltage.

DOI: 10.1103/PhysRevB.74.245308 PACS number(s): 72.20.−i, 72.30.+q, 73.20.Mf

I. INTRODUCTION

Studying single electron tunneling through a quantum dot (QD) reveals a series of fascinating phenomena, such as, charging effects,[1] Coulomb blockade (CB),[2–4] spin blockade (SB),[5] voltage-controlled spin polarization,[6] tunneling magnetoresistance (TMR),[7] quantum tunneling of magnetization,[8] and Kondo effects.[9] With the development of magnetic nanostructures, such as diluted magnetic semiconductor quantum dots (DMSQD), the control of spin-related phenomena on a nanoscale becomes possible.[10–31]An ability to incorporate a few magnetic Mn^{2+} ions into a controlled electronic environment, such as a self-assembled QD with tunable number of carriers, would make an important breakthrough in spintronics devices because it allows one to manipulate and detect individual spins, which plays a crucial role in spintronics and quantum information processing.[6,17–19]

Recently QDs with a single magnetic ion have been realized.[12–15] Optical emission spectra from single Mn^{2+} ion-doped II-VI QD (SMNQD) reveal the zero-field spin splitting of the exciton-Mn hybridized states due to the *sp-d* exchange interaction.[12–15] Moreover, the transport measurement through a DMSQD exhibits the splitting of the current even in the absence of an external magnetic field.[21] These electron-Mn exchange interaction induced energy splittings allow one selectively to bring the spin-up or spin-down state into resonance in transport measurement, resulting in a suppression of undesired spin channel and a dramatic enhancement of the transmission probability of the desired spin species.[6,21] Hence, DMSQDs can be operated as voltage-controlled spin filters to selectively inject carriers of desired spin into semiconductors from a ferromagnetic lead.[6,21] Moreover, this spin-dependent transport can be further tuned by the magnetization of the leads[7,28–31] and an external magnetic field.[4,29–32] Then a desired spin polarization of the current can be achieved by an appropriate choice of bias voltage, quantum confinement ω_0, Mn^{2+} ion positions, magnetization of the leads, and external magnetic field.

The facts and considerations mentioned above motivated us to develop a comprehensive theory of spin-dependent transport through a SMNQD weekly coupled to the leads, in the presence or absence of an external magnetic field, using the sequential tunneling approach and assuming that spin flips do not occur. The paper is organized as follows. In Sec. II we present the model of the Mn^{2+} ion-doped QD, in Sec. III various results, and in Sec. IV concluding remarks.

II. THEORETICAL MODEL

We study the transport properties of a Mn^{2+} ion-doped two-dimensional quantum dot weakly coupled to two reservoirs by tunneling barriers, as shown in Fig. 1, in the standard tunneling Hamiltonian approach. The Hamiltonian of the system is given by a sum of a reservoir and dot Hamiltonians and a tunneling term. The latter describes the transfer of electrons from the reservoir, where the Coulomb interaction between the electrons is effectively screened (metallic regime), to the quantum dot, where the Coulomb interactions between electrons and the electron-Mn^{2+}-ion exchange inter-

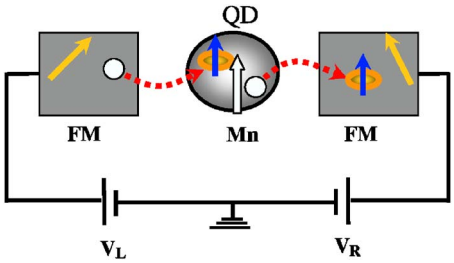

FIG. 1. (Color online) Geometry of a single-electron transistor (SET) composed of a left ferromagnetic lead, a Mn^{2+} ion-doped QD, and a right ferromagnetic or normal-metal lead. The orientations of the magnetization in the leads, indicated by the inclined (yellow) arrows, can be controlled independently. The spin of the Mn^{2+} ion is indicated by the white arrow, that of the electrons by the blue arrows, and the electron tunneling by the curved arrows.

action are most important. To enhance the spin-dependent transport, we use a small QD doped by a paramagnetic ion. Our results are based on features of the few-particle eigenstates of the dot Hamiltonian operator, which describes interacting electrons and exchange interaction between electrons and a magnetic ion in a parabolic confinement potential subjected to a perpendicular magnetic field B. Transport through such a QD occurs when the Fermi energy of the leads is aligned with one of the discrete energy levels of the confined region. The full Hamiltonian reads[29,30]

$$\hat{H} = \sum_{k,\sigma} \epsilon_{k,\sigma} \hat{a}^{+}_{k,\sigma} \hat{a}_{k,\sigma} + \sum_{p,\sigma} \epsilon_{p,\sigma} \hat{b}^{+}_{p,\sigma} \hat{b}_{p,\sigma} + \hat{H}_D + \hat{H}_T. \quad (1)$$

The first and second terms in $\hat{H}$ describe the free (L) and right (R) electrodes, where $\hat{a}^{+}_{k,\sigma}(\hat{a}_{k,\sigma})$ creates (destroys) an electron with momentum k in channel σ in the left lead, and $\hat{b}^{+}_{p,\sigma}(\hat{b}_{p,\sigma})$ operators for electrons in the right lead. The third term denotes the Hamiltonian of a quantum dot. Following Ref. 18 we write the many-electron single-Mn Hamiltonian in second quantization form. Denoting annihilation (creation) operators for electrons in the single-particle state i by $c_{i,\sigma}(c^{+}_{i,\sigma})$ and spin-raising (-lowering) operators in the Mn^{2+} ion by M^{+}, M^{-}, $\hat{H}_D$ can be written as

$$\begin{aligned}\hat{H}_D = & \sum_{i,\sigma} E_{i,\sigma} c^{+}_{i,\sigma} c_{i,\sigma} + (1/2) \sum_{i,j,k,l}^{\sigma\sigma'} \langle i,j|V_{ee}|k,l\rangle c^{+}_{i,\sigma} c^{+}_{j,\sigma'} c_{k,\sigma'} c_{l,\sigma} \\ & - (1/2) \sum_{i,j} J_{i,j}(R)[(c^{+}_{i,\uparrow} c_{j,\uparrow} - c^{+}_{i,\downarrow} c_{j,\downarrow}) M_z + c^{+}_{i,\downarrow} c_{j,\uparrow} M^{+} \\ & + c^{+}_{i,\uparrow} c_{j,\downarrow} M^{-}] - \mu_B B \sum_{i} [g_e S^{(i)}_z + g_{Mn} M_z]. \quad (2)\end{aligned}$$

The first line in Eq. (2) describes the spin-independent part of the electron Hamiltonian, with $E_{i,\sigma}$ the kinetic energy of an electron on the single-particle orbital $|i\rangle$ with spin σ and $\langle i,j|V_{ee}|k,l\rangle$ two-body Coulomb matrix elements. The second line describes the interaction of Mn^{2+} ions with electrons. The electron-Mn sp-d exchange interaction is modeled here by a contact ferromagnetic interaction $\hat{H}_{e\text{-Mn}} = -J^{2D}_C \vec{M} \cdot \vec{S} \delta(\vec{r} - \vec{R})$, where $\vec{S}$ ($\vec{M}$) is electron (Mn) spin, $\vec{r}$ ($\vec{R}$) is electron (Mn) position, and $J^{2D}_c = 2J_c/d$ with J_c the bulk exchange interaction strength and d thickness of the quantum dot. In second quantization form, it consists of three terms. The first term measures difference in spin-up and spin-down populations and acts as the electron Zeeman energy in the field of the magnetic ion as well as a source of electron spin-conserving scattering. The second and third term involve scattering accompanied by flipping of electron spin compensated by the flipping of Mn spin. The electron-Mn interaction strength is proportional to the electron-Mn exchange matrix elements $J_{ij}(R) = J^{2D}_C \varphi^{*}_i(R) \varphi_j(R)$ determined by the wave function of the two states "i" and "j" at the position R of the Mn^{2+} ion. For a small dot, it increases as V^{-1}, where V is the volume of the QD. Then it can be manipulated by changing the Mn ion position, modulating the QD size, and by varying the number of electrons in the QD. Hence the effect of Mn is to introduce a spin-related disorder. The last line in $\hat{H}_D$ is the Zeeman energy of the electron and Mn ion. Here $g_{\text{Mn}}(g_e)$ is the Mn (electron) g factor, μ_B is the Bohr magneton, and B the magnetic field along the z axis.

We consider a quasi-two-dimensional QD with parabolic confinement, a model suitable for self-assembled QDs.[17] The single-particle states and energies of an electron in such a QD are those of two coupled harmonic oscillators with quantum numbers n_+ and n_-, i.e., $E_e(n_+,n_-) = (n_+ + 1/2)\omega_+ + (n_- + 1/2)\omega_-$ forming twofold electronic shells with $\omega_\pm = (\omega_0^2 + \omega_c^2/4)^{1/2} \pm \omega_c/2$, $n_+(n_-) = 0,1,2,\ldots$; ω_0 characterizes the confining potential and ω_c is the cyclotron frequency. The corresponding eigenstates are $\varphi_{n_+,n_-}(x,y) = \varphi_{n_+}(x)\varphi_{n_-}(y)$.[9] The lowest three 1D harmonic oscillator states are $\varphi_0(\hat{x}) = e^{-\hat{x}^2/4}/(2\pi l_0^2)^{1/4}$, $\varphi_1(\hat{x}) = \hat{x} e^{-\hat{x}^2/4}/(2\pi l_0^2)^{1/4}$, and $\varphi_2(\hat{x}) = (\hat{x}^2 - 1)e^{-\hat{x}^2/4}/(8\pi l_0^2)^{1/4}$, with $\hat{x} = x/l_0$ and $l_0 = (\omega_0)^{-1/2}$. Here length and energy are measured in effective Bohr radius a_B and effective Rydberg (Ry). The ground state energy is determined by $E_e(0,0) = (\omega_+ + \omega_-)/2$. In what follows we adopt $J_c = 15$ eV Å^3, $d = 2$ nm, $\varepsilon = 10.6$, $m^* = 0.106$, Bohr radius $a_B = 5.29$ nm, Ry = 12.8 meV, $g_e = -1.67$, $g_{\text{Mn}} = 2.02$, applicable to II-VI (Cd,Mn)Te semiconductor QDs.[18,19] The spin-dependent hybridization $\hat{H}_T$ of the QD to the electrodes is given by

$$\begin{aligned}\hat{H}_T = & \sum_{k,i,\sigma} T^{L}_{k,i,\sigma} [\hat{a}^{+}_{k,\sigma} \hat{c}_{i,\sigma} + \hat{c}^{+}_{i,\sigma} \hat{a}_{k,\sigma}] + \sum_{p,i,\sigma} T^{R}_{p,i,\sigma} [\hat{b}^{+}_{p,\sigma} \hat{c}_{i,\sigma} \\ & + \hat{c}^{+}_{i,\sigma} \hat{b}_{p,\sigma}], \quad (3)\end{aligned}$$

where $T^{L/R}_{k,i,\sigma}$ are the transmission probability amplitudes. We assume that the electron spin is conserved in the tunneling process and the QD is weakly coupled to electrodes which are in thermal equilibrium with the left (L), right (R) reservoirs described by the Fermi-Dirac distributions $f_{L/R}(E) = \{1 + \exp[\beta(E - \mu_{L/R})]\}^{-1}$, where E is the difference between the energy of N_e-particle state i and $(N_e - 1)$-particle state i'. The Fermi-Dirac distribution function $f_{L/R}(E)$ characterizes the occupation of electron levels in the left (electrochemical potential μ_L) and right (μ_R) reservoir. The transmittance $t^{L/R}_\sigma = 2\pi |T^{L/R}_{k,j,\sigma}|^2 \rho^{L/R}_\sigma \Omega/\hbar$, is proportional to the square of the transmission probability amplitude of the barriers, can be different in the two leads; $\rho^{L/R}_\sigma$ denotes the electron density of states with spin σ in the $L(R)$ lead and Ω is the volume of the unit cell. For simplicity, they are assumed to be independent of energy.

To understand the underlying physics of spin-dependent tunneling, we introduce $t^{L}_\sigma = t_0(1 + \sigma\Delta_L)/2$ and $t^{R}_\sigma = \alpha t_0(1 + \sigma\Delta_R)/2$ where $\sigma = \pm 1$, the factor Δ_L (Δ_R) describes the spin selectivity of the contacts between the left (right) lead and the QD, t_0 is a parameter independent of the bias voltage V_{SD}, and α refers to the asymmetry between the right and left leads. Further, we assume that the SET is in the strong Coulomb blockade and sequential tunneling regime. Because of the large Coulomb blockade energy, the population number N_e of electrons can take on only the values 0 and 1. For $N_e = 1$, the spin-dependent part of $\hat{H}_D$ is given by $\hat{H}_{\text{spin}} = -J_{ss} \vec{S} \cdot \vec{M} - (g_e S_z + g_{\text{Mn}} M_z)\mu_B B$, where J_{ss} is the exchange in-

teraction strength in the electronic s shell. Since $[J_z, \hat{H}_{\text{spin}}]=0$, the eigenvalue m of J_z is a good quantum number, with $\vec{J}=\vec{S}+\vec{M}$ the total spin of the hybrid system. Hence, the eigenstates of the Hamiltonian $\hat{H}_{\text{spin}}$, characterized by m, take the form

$$|m\rangle^{(\pm)} = a_{m\downarrow}^{(\pm)}|\downarrow\rangle|m+1/2\rangle + b_{m\uparrow}^{(\pm)}|\uparrow\rangle|m-1/2\rangle; \quad (4)$$

here $|m| \leq 2$, $a_{m\downarrow}^{(\pm)}=\{[(M+1/2)^2-m^2]/[2\Delta m(\Delta m \mp m')]\}^{1/2}$, $b_{m\uparrow}^{(\pm)}=\mp(1/\sqrt{2})(1\mp m'/\Delta m)^{1/2}$, and $|\uparrow\rangle(|\downarrow\rangle)$ is the state of an electron with spin up (spin down). The corresponding energies, in units of J_{ss}, are

$$\tilde{E}(m,\lambda) = [1/2 - 2mg_{\text{Mn}}\tilde{B} + \lambda\Delta m]/2, \quad (5)$$

with $\lambda=\pm 1, \Delta m=[(M+1/2)^2+m'^2-m^2]^{1/2}$, $m'=m+(g_e-g_{\text{Mn}})\tilde{B}$, and $\tilde{B}=\mu_B B/J_{ss}$. For $m=\pm 3$, the energy are given by $\tilde{E}(\pm 3)=-[M\pm(g_e+g_{\text{Mn}})\tilde{B}]/2$ and the corresponding eigenvector by $|\pm 3\rangle=|\pm 1\rangle|m\mp 1/2\rangle$.

The transition rates between the zero-electron $|0,M_z\rangle$ and one electron $|1,m,\lambda\rangle$ states of the dot have been calculated to the lowest order in $\hat{H}_T$. Simultaneous transitions of two or more electrons are of higher order in $\hat{H}_T$ and are neglected. An electron that enters (leaves) the dot through the left (right) tunnel barrier induces transitions between the $|i\rangle$ and $|j\rangle$ states and provides the energy difference $\Delta E(m,\lambda)=E_j-E_i$. The matrix elements describing these transitions are

$$\langle j|\hat{c}_\sigma^+|i\rangle = a_{m,\downarrow}^{(\pm)*}\delta_{\sigma,\downarrow}\delta_{M_z,m+1/2} + b_{m,\uparrow}^{(\pm)*}\delta_{\sigma,\uparrow}\delta_{M_z,m-1/2} \quad (6)$$

For an electron entering the QD, E_i is the Zeeman energy of magnetic ion, while E_j is the energy of the hybrid system. The transition matrix accounts for the combination of the spin of the incoming or leaving electron with the spin of the initial dot state to the spin of the final dot state and introduces spin selection rules. The magnetic quantum number m can be changed only by $\pm 1/2$ when one electron enters or leaves the dot. One finds the transition rates $\Gamma_{j,i}^{L/R}(\sigma,\lambda)$, from state i to state j in the presence of the coupled magnetic leads, in the form

$$\Gamma_{j,i}^{L/R}(\sigma,\lambda) = t_\sigma^{L/R}[|a_{m,\downarrow}^{(\pm)*}|^2\delta_{\sigma,\downarrow}\delta_{M_z,m+1/} + |b_{m,\uparrow}^{(\pm)*}|^2\delta_{\sigma,\uparrow}\delta_{M_z,m-1/2}] \times (f_{L/R}[\Delta E(m,\lambda)-\mu_{L/R}]\delta_{n_j,n_i+1} + 1 - f_{L/R}[\Delta E(m,\lambda)-\mu_{L/R}]\delta_{n_j,n_i-1}). \quad (7)$$

Hence the selection rules for the allowed transitions are $\delta m=\pm 1/2$ and $\delta M_z=0$, as shown in Fig. 2. Since Eq. (7) is an analytical expression, the calculation of the transition rates is straightforward using the expressions for $a_{m\downarrow}^{(\pm)}$, $b_{m\uparrow}^{(\pm)}$, and $\Delta E(m,\lambda)=E_j-E_i$, given between Eqs. (4) and (7). Details about $t_\sigma^{L/R}$ are given in Sec. III. As for $\mu_{L/R}$, one takes, e.g., $\mu_R=0$ and equates μ_L to the bias voltage.

The matrix elements of the total transition rates, for electrons with spin σ, between the states of the isolated dot are given by

$$\Gamma_{j,i}(\sigma) = \sum_\lambda [\Gamma_{j,i}^L(\sigma,\lambda) + \Gamma_{j,i}^R(\sigma,\lambda)]. \quad (8)$$

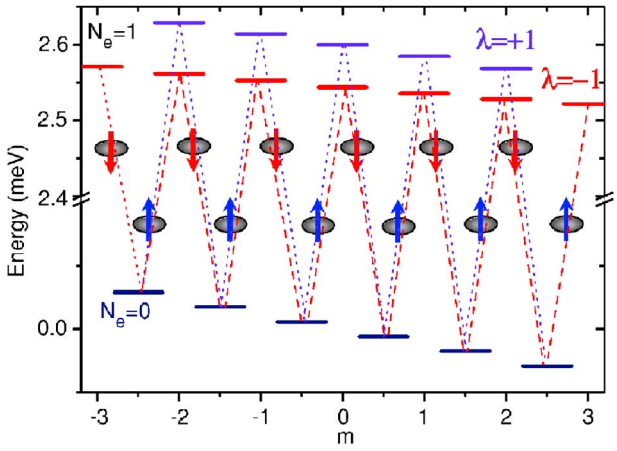

FIG. 2. (Color online) Scheme of the energy levels of a Mn^{2+} ion-doped QD in an external magnetic field versus magnetic quantum number m. All allowed transitions, involving the states with $N_e=0$ and $N_e=1$ electrons, and the corresponding electron spins are shown. The red and violet sublevels are associated with the $\lambda=-1$ and $\lambda=+1$ channel, respectively.

The probability P_i of finding the QD in the state i will deviate from its equilibrium value for a given drain-source voltage $V_{\text{SD}}=(\mu_L-\mu_R)/e$. Its dependence on the tunneling rate $\Gamma_{j,i}$ is well described by kinetic equations. The stationary nonequilibrium populations P_i obey the Master equation

$$\sum_{j(j\neq i)} [\Gamma_{i,j}(\sigma)P_j - \Gamma_{j,i}(\sigma)P_i] = 0. \quad (9)$$

This is a set of linear equations whose number is equal to the number of states (N_S) in the dot. For computational purposes we rewrite it in the form

$$\sum_{j=1}^{N_s} \Pi_{i,j}(\sigma)P_j = 0 \quad (10)$$

with the matrix $\Pi_{i,j}$ given by

$$\Pi_{i,j} = \Gamma_{i,j} - \delta_{i,j}\sum_{l=1}^{N_s}\Gamma_{l,j}(\sigma). \quad (11)$$

To satisfy the normalization condition ($\Sigma_{j=1}^{N_S}P_j=1$), one sets $\Pi_{1,j}=1$ and uses $\Sigma_{j=1}^{N_S}\Pi_{i,j}(\sigma)P_j=\delta_{1,i}$ to calculate the stationary occupation probability.

Knowing the stationary probability P_j from the Master equation, the spin-polarized current I_σ is calculated by

$$I_\sigma = e/2\sum_{i,j(j\neq i)} [\Gamma_{i,j}^L(\sigma) - \Gamma_{j,i}^R(\sigma)](N_j - N_i)P_j. \quad (12)$$

It equals the number of electrons with spin σ that pass through the left or right barrier per unit time. To measure the dependence of I_σ on V_{SD}, we define the spin polarization ratio $\eta=(I_\uparrow-I_\downarrow)/(I_\uparrow+I_\downarrow)$ and its λ component $\eta^{(\lambda)}=(I_\uparrow^{(\lambda)}-I_\downarrow^{(\lambda)})/(I_\uparrow^{(\lambda)}+I_\downarrow^{(\lambda)})$ for all allowed transitions, where $I_\sigma^{(\lambda)}$ is the spin-polarized current through the λ channel. The tunnel current is the sum of the currents carried by spin-up and spin-down electrons: $I(\lambda)=I_\uparrow(\lambda)+I_\downarrow(\lambda)$.

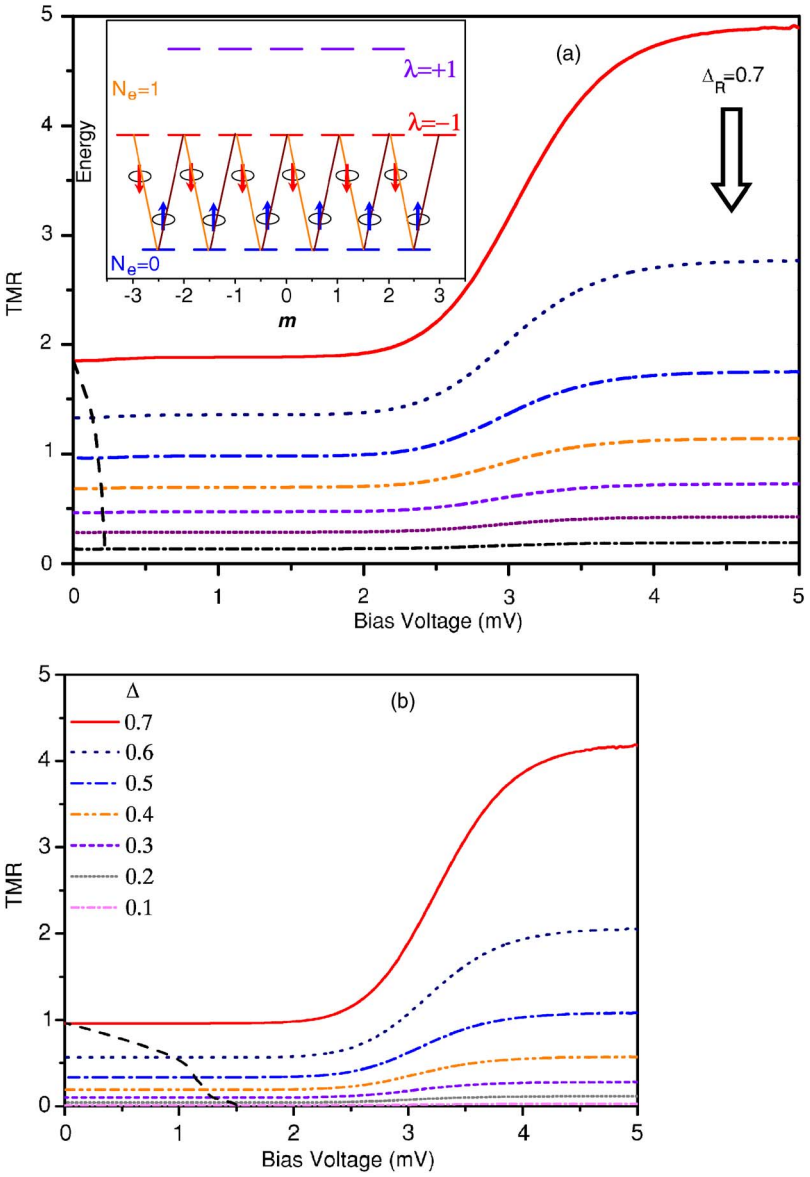

FIG. 3. (Color online) Voltage dependence of the TMR at $T=4$ K and $B=10^{-4}$ T for asymmetric leads with $\alpha=0.6$, $\Delta_L=0.9$ (a) and for symmetric leads with $\alpha=1$ and $\Delta_L=\Delta_R=\Delta$ (b) for several values of Δ_R. The dashed black curves show the TMR of the corresponding undoped QD and separate the regions of enhanced (to their right) and suppressed (to their left) TMR. As the white arrow indicates, Δ_R decreases downwards (in steps of $\delta\Delta_R=0.1$). The inset in (a) shows a scheme of the energy levels for the $N_e=0$ and $N_e=1$ multiplets without external magnetic field.

The differential conductance is defined by $G\equiv dI/dV$ and the TMR by $\mathrm{TMR}=(G_{\mathrm{FM}}-G_{\mathrm{AF}})/G_{\mathrm{AF}}$, where G_{AF} and G_{FM} denote the total conductances in the antiparallel (AF) and parallel (FM) alignment of the magnetization in the left and right leads ($G_k=G_k^{\uparrow}+G_k^{\downarrow}, k=\mathrm{FM},\mathrm{AF}$). Further, we assume $t_{\pm}^R=\alpha t_0(1\pm\Delta_R)/2$, for the ferromagnetic (FM) alignment, and $t_{\pm}^R=\alpha t_0(1\mp\Delta_R)/2$ for the antiferromagnetic one (AF). For comparison, we also derive the corresponding expressions for an undoped quantum dot $\eta=(I_+^{(e)}-I_-^{(e)})/(I_+^{(e)}+I_-^{(e)})$ and $\mathrm{TMR}=-1+(\Sigma_{j=-1}^{+1}A_j^+)/(\Sigma_{j=-1}^{+1}A_j^-)$, with $I_\sigma^{(e)}=t_\sigma^L t_\sigma^R/[t_\sigma^L+t_\sigma^R]$ and $A_j^{\pm}=(1+j\Delta_L)(1\pm j\Delta_R)/[(1+j\Delta_L)+\alpha(1\pm j\Delta_R)]$. We notice that both η and the TMR depend only on the tunneling parameters of the leads. For instance, $\eta=\Delta$ and $\mathrm{TMR}=\Delta^2/(1-\Delta^2)$, for two symmetric leads with $\Delta_L=\Delta_R=\Delta$ and $\alpha=1$. For a SET composed of two symmetric leads, e.g., one spin-polarized left lead and a normal-metal right lead, we have $\eta=\Delta_L/(2-\Delta_L^2)$ and $\mathrm{TMR}=0$ assuming that $\alpha=1$.

III. RESULTS AND DISCUSSION

A. Spin-dependent transport through a QD in an external magnetic field

The TMR of a SMNQD depends strongly on V_{SD}, the transmittances of the barriers, the relative orientation of the magnetization between the electrodes, the strength of the electron-Mn exchange interaction J_{ss}, and the tunneling strength t_0. Typical values of J_{ss} and t_0 are of the order of a few hundreds and a few tens of μeV, respectively.[33] Figure 3 shows the voltage dependence of the TMR of a SMNQD at $T=4$ K and $B=10^{-4}$ T for asymmetric leads, with $\alpha=0.6$, $\Delta_L=0.9$ (a) and for symmetric leads with $\alpha=1$ and $\Delta_L=\Delta_R=\Delta$ (b) for several values of Δ_R. For comparison, the corresponding TMRs of an undoped QD are also shown by the (black) dashed curves. The TMR increases to their right and decreases to their left. We find that the TMR increases with increasing either applied bias voltage or spin selectivity Δ_R.

Moreover, it is strongly enhanced by the electron-Mn exchange interaction, as shown in the region located to the right of the lines corresponding to the undoped QD. The underlying physics is the following. At low bias voltage the current is thermally suppressed by CB. With increasing bias voltage, the transitions between the $N_e=0$ multiplets and the states of the $\lambda=-1$ channel become energetically allowed as long as electrons in the left lead have enough energy to overcome the energy barrier between the $N_e=0$ and $N_e=1$ states. According to the selection rule for sequential tunneling, both spin-up and spin-down electrons can hop into the QD from the left lead but with different rates due to the different densities of states at the Fermi level for majority and minority spin states in the incoming lead. For two leads ferromagnetically aligned, outgoing spin-up electrons leave the QD much faster than the spin-down ones, except when electron spin-flip processes occur and the local spin is simultaneously changed by unity. However, the number of possible spin flips is very limited. Then, one can neglect spin relaxation.[6] Hence the current is spin polarized and increases with applied bias voltage beyond a threshold voltage. In contrast, when the two leads are anti-ferromagnetically aligned, the majority spin electrons in the right lead are with spin down. Then spin-up electrons leave the QD much slower than the spin-down ones. On the other hand, the large spin selectivity ΔR enlarges the difference in the density of states between spin-up and spin-down electrons. Hence, a positive TMR is expected and it is enhanced with increasing Δ_R.

The effect of the electron-Mn exchange interaction on TMR can be understood in the following way. An injected electron from the left lead polarizes the spin of the Mn^{2+} ion. In turn, the magnetic field induced by the polarized Mn^{2+} ion orientates the spin of the electron. Finally, the exchange interaction between electron and Mn^{2+} ion in the QD results in a parallel alignment of spins of the electron and Mn^{2+} ion in the ground state of the hybrid system. It facilitates the tunneling of the electrons with spin-up, but impairs the tunneling of spin-down electrons, resulting in an enhanced TMR. In addition, the TMR is also strongly affected by the symmetry between the right and left leads. Figure 4 shows the dependence of TMR on the bias voltage for asymmetric leads with $\Delta_L=\Delta_R=0.5$ at several values of α. When α is increased from 0.6 to 2.0, the TMR decreases dramatically.

The strength of the exchange interaction between an electron and a Mn^{2+} ion is proportional to the square of the electron wave function at the paramagnetic ion. Thus for a fixed position of Mn^{2+} ion, e.g., located at the center of the QD, the electron-Mn exchange interaction increases with increasing quantum confinement ω_0, resulting in a larger separation between electronic sublevels. Consequently, the larger ω_0, the more pronounced the Coulomb blockade, as shown in Fig. 5. The inset in Fig. 5 shows the differential conductance for the current with spin up and spin down, as indicated by the direction of the arrows. Note that the conductance for current with spin up is one order of magnitude larger than that for current with spin down and that the two conductance peaks are separated.

An external magnetic field tilts the energy levels of an electron and a single Mn hybrid system with respect to the magnetic quantum number m due to the additional Zeeman

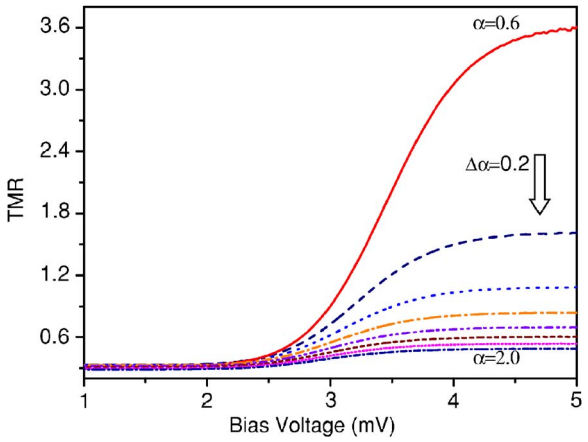

FIG. 4. (Color online) Voltage dependence of the TMR at $T=4$ K and $B=10^{-4}$ T for asymmetric leads with $\Delta_L=\Delta_R=0.5$ and several values of α increasing downwards from 0.6 to 2.0 in steps of $\Delta\alpha=0.2$.

energy. It removes the degeneracy of the spin multiplets, as shown in Fig. 2. In the small magnetic filed regime ($\tilde{B}<1$), the sublevel with total spin $J=3$ and magnetic quantum number $m=3$ possesses the lowest energy. With increasing magnetic field, the Zeeman energy increases considerably, but the electron-Mn exchange interaction is only slightly affected. For $\tilde{B}>1$ the Zeeman energy exceeds the electron-Mn exchange interaction energy and dominates the energy spectrum. In the strong magnetic field limit, $\tilde{B}\gg 1$, $m'=m+(g_e-g_{\mathrm{Mn}})\tilde{B}$, $\Delta m=-m'$. The exchange interaction between an electron and the Mn^{2+} ion can be safely neglected. Then the electronic states of the hybrid system are well described by $|\sigma\rangle|M_z\rangle$. The energy levels are given by $\tilde{E}_\sigma(m)=-[\sigma g_e+(m-\sigma)g_{\mathrm{Mn}}]\tilde{B}$, where $m=\sigma/2+M_z$. According to the value of σ, they are classified by two groups. One is composed of the states $|+1\rangle|M_z\rangle$ and the other of the states $|-1\rangle|M_z\rangle$. The

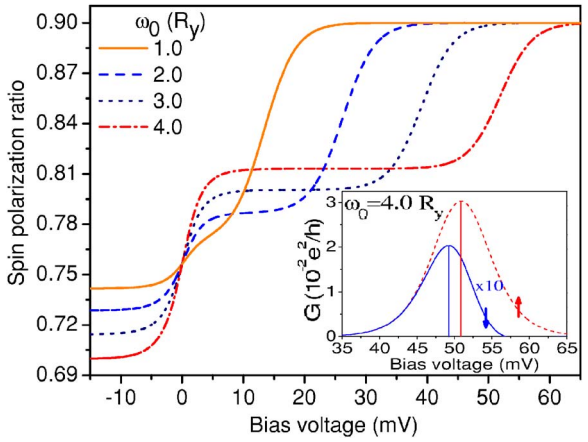

FIG. 5. (Color online) Dependence of the spin polarization on the bias voltage for several values of ω_0. The parameters assumed are $\alpha=1.0$, $\Delta_L=0.9$, $\Delta_R=0.0$, $T=30$ K, and $B=10^{-4}$ T. The inset shows the differential conductance G as a function of the bias voltage for $\omega_0=4.0$ Ry; the direction of the spin is indicated by an arrow.

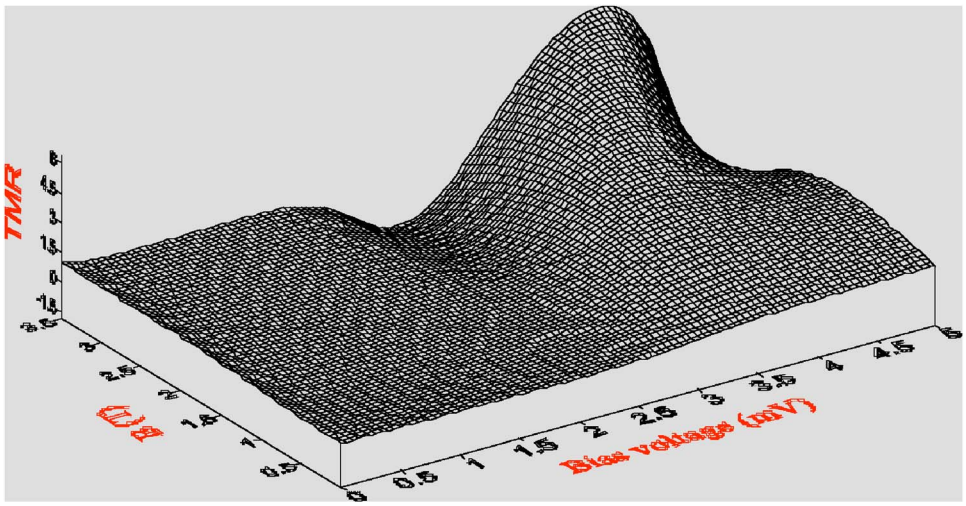

FIG. 6. (Color online) Tunneling magnetoresistance as a function of the magnetic field and of the bias voltage for $T=4$ K, $\alpha=1$, and $\Delta_L=\Delta_R=0.5$.

state with $\sigma=-1$ and $m=2$ becomes the ground state. Figure 6 shows a surface plot of the TMR as a function of the magnetic field and bias voltage at $T=4$ K, $\alpha=1$, and $\Delta_L=\Delta_R=0.5$. In the small magnetic field regime and for low temperatures, the current is suppressed due to the CB for small bias voltages. With increasing bias voltage, the energy levels drop into the window of the bias voltage successively. Hence, beyond the CB regime, the current as well as the TMR increase with increasing bias voltage. On the other hand, the Zeeman splitting increases with increasing magnetic field. For strong magnetic fields ($\tilde{B}\gg 1$), the interplay between the magnetic field and the bias voltage gives rise to an oscillatory TMR. The underlying physics is as follows. With increasing bias voltage, the transitions involving an electron with spin down take place as long as the energy difference between the ground state of the $N_e=0$ multiplet with $m=M$ and the lowest-energy state of the $N_e=1$ multiplet with $m=M-1/2$ becomes energetically allowed; these is a minority-spin involved transition. With a further increasing bias voltage, the majority-spin involved transitions between the state $|0,M\rangle$ and the state of the $N_e=1$ multiplet with $m=M+1/2$ occur. After that, the other spin-up and spin-down tunneling channels are successively activated. The result is an oscillatory spin polarization as well as an oscillatory TMR. This oscillatory behavior changes when the relative orientation of the magnetization changes and points to applications in magnetic sensors.

To clarify the essential physics of spin-dependent transport through a Mn^{2+} ion doped QD, we derive an analytical expression for spin-polarized current in a one-band model, assuming that, in a certain magnetic-field range, only a transition between the state $|0,-5/2\rangle$ and $|1,-2,-1\rangle$ is energetically allowed. For brevity, one denotes the former (later) state by 1 (2). The occupation probability satisfies the detailed balance equation $\Gamma_{1,2}P_2=\Gamma_{2,1}P_1$, where $\Gamma_{1,2}^{L/R}=t_{\uparrow}^{L/R}(1-f_{L/R})$, $\Gamma_{2,1}^{L/R}=t_{\uparrow}^{L/R}f_{L/R}$ and $\Gamma_{i,j}=\Gamma_{i,j}^{L}+\Gamma_{i,j}^{R}$. Then the spin-polarized current is $I_{\uparrow}/I_0^{\uparrow}=f_R-f_L$, where $I_0^{\uparrow}=(e/2)[\alpha t_0(1+\Delta_L)(1+\Delta_R)]/[2(1+\Delta_L)+\alpha(1+\Delta_R)]$ only depends on the lead properties. Hence the spin-polarized current is determined by the applied voltage and lead properties. Let us first study the effects of the magnetization of the leads, reflected by Δ_L and Δ_R, on the current. For a SET comprised of one ferromagnetic left lead and a normal-metal right lead, we have $I_0^{\uparrow}=(e/2)t_0/[\alpha^{-1}+(1+\Delta_L)^{-1}]$. Hence an increase of either α or Δ_L gives rise to an increased spin-polarized current. A similar behavior is noted for a SET composed of two parallel-aligned ferromagnetic leads. However, an opposite Δ_L dependence is found in a SET with two antiparallel-aligned ferromagnetic leads, e.g., $I_0^{\uparrow}=(e/4)(1-\Delta_L^2)t_0$ for $\Delta_L=\Delta_R$ and $\alpha=1$. It is interesting to note that for $\Delta_L=1$, the current of electrons is completely suppressed. Let us now turn to the influence of the applied bias voltage on the current. Using the relation $df/d\varepsilon=-\cosh^2(\varepsilon/2k_BT)/4k_BT$, one derives $I_{\uparrow}/I_0^{\uparrow}=\Theta(\mu_L-\Delta E)-\Theta(\mu_R-\Delta E)$, for $k_BT<V_{SD}$, and $I_{\uparrow}/I_0^{\uparrow}=(V_{SD}/4k_BT)\cosh^{-2}[(\Delta E-\mu_L/2k_BT)]$ for $k_BT>V_{SD}$. Hence the system works as an almost perfect spin valve even though the ferromagnetic leads are not half metallic.

B. Voltage-controlled spin filters

One challenge in spintronics is the source of spin injection. To illustrate the mechanism of voltage-controlled spin filtering, let us focus on the electronic transport through the Mn^{2+} ion doped QD in the absence of magnetic filed. In this case, $m'=m$, $\Delta m=M+1/2$, and the Hamiltonian $\hat{H}_{\text{spin}}$ turns out to be $\hat{H}_{\text{spin}}=-J_{ss}\vec{S}\cdot\vec{M}$. The exchange coupling between an electron and a Mn^{2+} ion splits the energy of hybrid system into two sublevels $\tilde{E}(\lambda=1)=(M+1)/2$ for $J=2$ and $\tilde{E}(\lambda=-1)=-M/2$ for $J=3$, as shown in the inset of Fig. 3. The correspondent states are $a_{m,\downarrow}^{(\lambda)}=(1/\sqrt{2})[1+m\lambda/(M+1/2)]^{1/2}$, $b_{m,\uparrow}^{(\lambda)}=-(1/\sqrt{2})[1-m\lambda/(M+1/2)]^{1/2}$. $|\uparrow\rangle|5/2\rangle$ and $|\downarrow\rangle|-5/2\rangle$ are the wave functions related to $m=3$ and $m=-3$, respectively. Hence the states with energy $\tilde{E}(\lambda=1)[\tilde{E}(\lambda=-1)]$ are degenerated states with fivefold (sevenfold) degeneracy. Their separation is $E_{\text{ex}}=3J_{ss}$. For lower bias voltage, all transitions from the states of $N_e=0$ to the states of $N_e=1$ are thermally suppressed due to CB, while for a bias voltage is larger than $\tilde{E}(\lambda=-1)$ and less than $\tilde{E}(\lambda=1)$, only a single energy difference is relevant and all the relevant transitions become fully active.

Using $|\langle\sigma,M_z|1,m,\lambda\rangle|^2=(1-m\sigma\lambda/(M+1/2))/2$ we obtain the transition rate associated with the λ sublevel

$$\Gamma_{j,i}^{L/R}(\sigma,\lambda)=\frac{t_\sigma^{L/R}}{2}\left[\left(1+\frac{m\lambda}{M+1/2}\right)\delta_{\sigma,\downarrow}\delta_{M_z,m+1/2}+\left(1-\frac{m\lambda}{M+1/2}\right)\delta_{\sigma,\downarrow}\delta_{M_z,m-1/2}\right]\{f(J_{ss}M_\lambda/4-\mu_{L/R})\delta_{n_j,n_i+1}+[1-f(J_{ss}M_\lambda/4-\mu_{L/R})]\delta_{n_j,n_i-1}\},\tag{13}$$

where $M_\lambda=1+\lambda+2M$. Substituting the expressions of the transition-rate matrix elements $\Gamma_{ji}^{L/R}(\sigma,\lambda=1)$ and $\Gamma_{ji}^{L/R}(\sigma,\lambda=-1)$ in the Master equation, one notices that the occupation probability satisfies the detailed balance equation $P_{M_z}\xi_\sigma=P_m\zeta_\sigma$, which ensures equal formation rates of the populated m states from the unpopulated M_z state plus a σ electron, where $m=\sigma+M_z$, $\xi_\sigma=\Sigma_{k=L,R}t_\sigma^k f[\Delta E(m,\lambda)-\mu_k]$ and $\zeta_\sigma=\Sigma_{k=L,R}t_\sigma^k\{1-f[\Delta E(m,\lambda)-\mu_k]\}$ with $M_z=\pm5/2,\pm3/2,\pm1/2$. The analytical results for the occupation probability can be found from the solution of the detailed-balance equation. They are $P_m=P_0\chi_{1/2}^m$ and $P_{M_z}=P_0(\xi/\zeta)\chi_{1/2}^{2\sigma m}$, where $\chi_\sigma=\xi_\sigma\zeta_{-\sigma}/\xi_{-\sigma}\zeta_\sigma$. It is interesting to note that $P_mP_{-m}=P_0^2$ and $\chi_{-\sigma}=1/\chi_\sigma$. Then the spin-polarized current can be calculated by $I_\sigma(\lambda)=(e/2)\Sigma_{i,j(i\neq j)}[(t_\sigma^L f_L-t_\sigma^R f_R)(P_i+P_j)-(t_\sigma^L-t_\sigma^R)P_j]|\langle\sigma,M_Z|1,m,\lambda\rangle|^2$. After some algebra we find $I_\sigma(\lambda)=e\bar{P}(f_L-f_R)(t_\sigma^Lt_\sigma^R/2\zeta_\sigma)[1-\lambda\sigma M_J/(M+1/2)]$, where $\bar{P}=\Sigma_mP_m$, and M_J is the magnetization of the populated states in terms of the Brillouin function $B_J(x)$, given by $M_J=B_J(\ln\chi_{1/2})$. $I_\sigma(\lambda)$ shows that the effect of the paramagnetic ion on the spin-polarized current through the dot is completely described in terms of the magnetization of the dot in the populated state. It also allows one to find the dependence of the λ component of the spin polarization ratio $\eta(\lambda,M_J)=\Gamma_0[1-\lambda\Gamma_0^{-1}M_J/(M+1/2)]/[1-\lambda\Gamma_0M_J/(M+1/2)]$, where $\Gamma_0=(\alpha\Delta_L+\beta\Delta_R)/(\alpha+\beta)$, and $\beta=(1-\Delta_L^2)f_L/(1-\Delta_R^2)f_R$. The parameter Γ_0 depends only on the lead properties and applied bias voltage, describing the spin selectivity of the dot for small currents and $M_J\ll J$.

To study the spin-injection from a ferromagnetic lead to semiconductor materials, utilizing a SET comprised of a left FM lead and a right normal-metal lead or a semiconductor ($\Delta_R=0$), one gets $\Gamma_0=\alpha\Delta_L/[\alpha+(1-\Delta_L^2)f_L/f_R]$. For small bias voltages, $f_L\to f_R$, $\chi_{1/2}=1$, and the magnetization $M_J\to0$. If $M_J/J\to0$, the polarization ratio equals Γ_0, for both values of λ, and $\Gamma_0<\Delta_L$. Therefore, an unpolarized ion suppresses spin injection. The ratio Γ_0/Δ_L depends on the ratio of the transmittance of the contacts and, when the difference in the transmittance between the left and the right leads is much larger than 1, the suppression is strong. However, M_J grows quickly with increasing voltage while Γ_0 decreases slowly. When M_J becomes larger than $\Gamma_0(M+1/2)$, the spin injection blockade breaks down and the polarization ratio acquires its normal magnitude $\eta(\lambda)\approx\Delta_L$. The stronger the suppression of Γ_0, the narrower is the range of voltages in which the "spin injection blockade" occurs. In this range of parameters, the dot behaves as a highly nonlinear spin emitter.

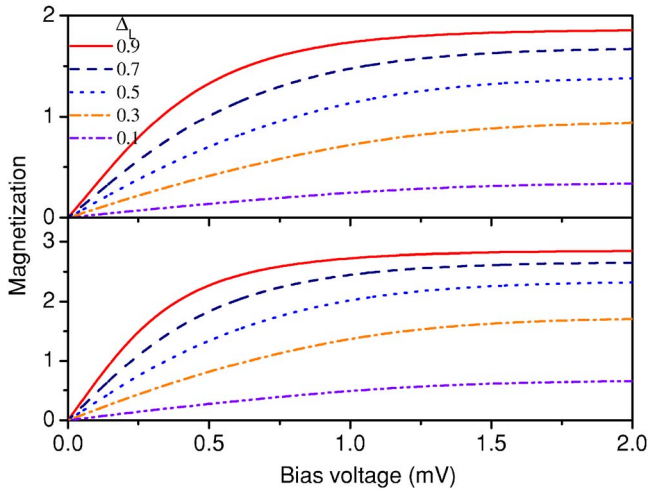

FIG. 7. (Color online) Dependence of the magnetization on bias voltage for different values of Δ_L with $J=2$ (upper panel) and $J=3$ (lower panel), calculated through $M_J=B_J\ln(\chi_{1/2})$. The parameters assumed are $\alpha=1.0$, $\Delta_R=0.0$, $T=4$ K and $B=0.0$ T.

The dependence of the magnetization on the bias voltage at different values of Δ_L for $\lambda=1$ (upper panel) and $\lambda=-1$ (lower panel), calculated through $M_J=B_J\ln(\chi_{1/2})$ and by assuming $\alpha=1.0$, $\Delta_R=0.0$, $T=4$ K, and $B=0.0$ T, is shown in Fig. 7. The magnetization increases with increasing voltage. When the voltage is zero, the magnetization vanishes for both values of λ. This implies that the magnetization is induced by a spin-polarized current. In addition, the magnetization can be enhanced by a large J and a high spin selectivity. Figure 8 shows the spin polarization ratio of the λ component calculated through the analytical expression of $\eta(\lambda,M_J)$ for $J=2$ (dashed lines) and $J=3$ (solid lines) (a) and the spin polarization ratio obtained by numerical calculations (b) vs bias voltage at $T=4$ K and $B=0$ T for a single Mn^{2+}-ion doped QD with different values of Δ_L. The parameters assumed are $\alpha=1.0$, $\Delta_R=0.0$. The two components $\eta(\lambda=+1)$ and $\eta(\lambda=-1)$ of the spin polarization present opposite behaviors with increasing bias voltage, e.g., $\eta(\lambda=-1)$ increases with voltage while $\eta(\lambda=+1)$ decreases and can even change sign. For comparison, the spin polarization of the current in an undoped QD. i.e., without the Mn^{2+} ion, is presented by the dashed black curve. We notice that the electron-Mn exchange interaction can strongly enhance the spin polarization of the current, as shown in the region to the right of the dashed black curve. This behavior can be observed in both Figs. 8(a) and 8(b).

IV. CONCLUDING REMARKS

A quantum theory of single electron tunneling through single Mn^{2+} ion doped II-VI quantum dot weakly coupled to one ferromagnetic and one nonmagnetic/ferromagnetic leads in the Coulomb blockade regime has been developed.[1,2] Analytical expressions for the magnetization, spin-dependent current, and spin polarization have been derived for zero

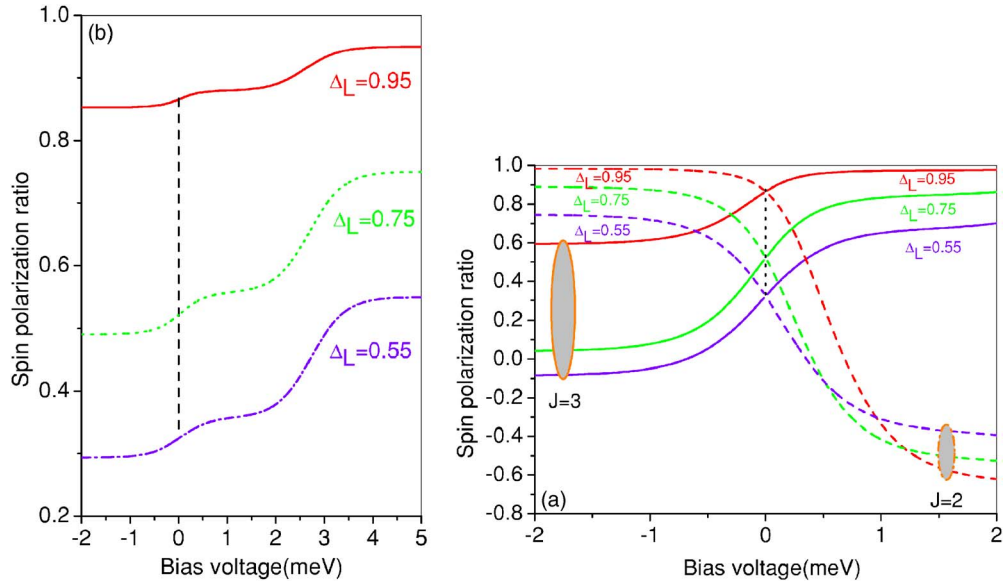

FIG. 8. (Color online) Spin polarization of the λ component calculated from the analytical expression of $\eta(\lambda, M_J)$ for $J=2$ (dashed curves) and $J=3$ (solid curves) (a) and obtained numerically (b) vs bias voltage at $T=4$ K and $B=0.0$ T for a single Mn^{2+}-ion doped QD with different values of Δ_L. The dashed black curves show the spin polarization for an undoped QD and separate the regions of enhanced (to their right) and suppressed (to their left) spin injection. The parameters used are $\alpha=1.0$, $\Delta_R=0.0$.

magnetic field. They predict a spin-injection-induced magnetization and a spin-polarized current. The numerical results show that the spin polarization and tunneling magntoresistance (TMR) strongly depend on the bias voltage V_{SD}, the spin selectivity of the leads, and the quantum confinement expressed by ω_0. Depending on V_{SD}, they can be strongly enhanced or weakened by the electron-Mn exchange interaction. An appropriate choice of V_{SD}, ω_0, and of the magnetization of the leads can yield a highly spin-polarized current even when the FM source is not 100% polarized.

In addition, an external magnetic field also impacts on the spin-dependent transport properties. For low magnetic fields, the spin polarization and the TMR increase monotonically with V_{SD} beyond the Coulomb blockade regime. When subjected to a strong magnetic field, an oscillatory behavior of the TMR with V_{SD} is predicted. Important applications of the theory are expected in voltage-controlled spin filters and magnetic sensors.

ACKNOWLEDGMENTS

This work was supported by the Canadian NSERC Grant No. OGP0121756. One of us (F.Q.) thanks P. Hawrylak and A. O. Govorov for valuable discussions.

*Electronic address: drfanyao@yahoo.com.br
†Electronic address: takis@alcor.concordia.ca

[1] R. M. Potok, J. A. Folk, C. M. Marcus, V. Umansky, M. Hanson, and A. C. Gossard, Phys. Rev. Lett. **91**, 016802 (2003).
[2] D. Pfannkuche and S. E. Ulloa, Phys. Rev. Lett. **74**, 1194 (1995).
[3] K. Jauregui, W. Häusler, D. Weinmann, and B. Kramer, Phys. Rev. B **53**, R1713 (1996).
[4] P. Recher, E. V. Sukhorukov, and D. Loss, Phys. Rev. Lett. **85**, 1962 (2000).
[5] D. Weinmann, W. Hausler, and B. Kramer, Phys. Rev. Lett. **74**, 984 (1995).
[6] A. L. Efros, M. Rosen, and E. I. Rashba, Phys. Rev. Lett. **87**, 206601 (2001).
[7] S. Takahashi and S. Maekawa, Phys. Rev. Lett. **80**, 1758 (1998).
[8] G.-H. Kim and T.-S. Kim, Phys. Rev. Lett. **92**, 137203 (2004).
[9] J. Park, A. N. Pasupathy, J. I. Goldsmith, C. Chang, Y. Yaish, J. R. Petta, M. Rinkoskie, J. P. Sethna, H. D. Abruna, P. L. McEuen, and D. Ralph, Nature (London) **417**, 722 (2002).
[10] S. C. Erwin, Lijun Zu, M. I. Haftel, A. L. Efros, T. A. Kennedy, and David J. Norris, Nature (London) **436**, 91 (2005).
[11] P. Hawrylak, M. Grabowski, and J. J. Quinn, Phys. Rev. B **44**, 13082 (1991).
[12] L. Besombes, Y. Léger, L. Maingault, D. Ferrand, H. Mariette, and J. Cibert, Phys. Rev. Lett. **93**, 207403 (2004).
[13] L. Besombes, Y. Leger, L. Maingault, D. Ferrand, H. Mariette, and J. Cibert, Phys. Rev. B **71**, 161307(R) (2005).
[14] Y. Léger, L. Besombes, L. Maingault, D. Ferrand, and H. Mariette, Phys. Rev. Lett. **95**, 047403 (2005).
[15] Y. Léger, L. Besombes, L. Maingault, D. Ferrand, and H. Mariette, Phys. Rev. B **72**, 241309(R) (2005).
[16] A. M. Yakunin, A. Yu. Silov, P. M. Koenraad, J. H. Wolter, W. Van Roy, J. De Boek, J. M. Tang, and M. E. Flatté, Phys. Rev. Lett. **92**, 216806 (2004).
[17] A. O. Govorov, Phys. Rev. B **70**, 035321 (2004) A. O. Govorou and A. V. Kalameitsev, *ibid.* **71**, 035338 (2005).
[18] F. Qu and P. Hawrylak, Phys. Rev. Lett. **95**, 217206 (2005).

[19] F. Qu and P. Hawrylak, Phys. Rev. Lett. **96**, 157201 (2006).
[20] J. Fernández-Rossier and L. Brey, Phys. Rev. Lett. **93**, 117201 (2004).
[21] C. Gould, A. Slobodskyy, T. Slobodskyy, P. Grabs, D. Supp, P. Hawrylak, F. Qu, G. Schmidt, and L. W. Molenkamp, cond-mat/0501597.
[22] D. M. Hoffman, B. K. Meyer, A. I. Ekimov, I. A. Merkulov, A. L. Efros, M. Rosen, G. Couino, T. Gacoin, and J. P. Boilot, Solid State Commun. **114**, 547 (2000).
[23] I. A. Merkulov, D. R. Yakovlev, A. Keller, W. Ossau, J. Geurts, A. Waag, G. Landwehr, G. Karczewski, T. Wojtowicz, and J. Kossut, Phys. Rev. Lett. **83**, 1431 (1999).
[24] J. Seufert, G. Bacher, M. Scheibner, A. Forchel, S. Lee, M. Dobrowolska, and J. K. Furdyna, Phys. Rev. Lett. **88**, 027402 (2002).
[25] A. Hundt, J. Puls, and F. Henneberger, Phys. Rev. B **69**, 121309(R) (2004).
[26] S. Mackowski, T. Gurung, T. A. Nguyen, H. E. Jackson, L. M. Smith, G. Karczewski, and J. Kossut, Appl. Phys. Lett. **84**, 3337 (2004).
[27] A. K. Bhattacharjee and C. Benoit á la Guillaume, Phys. Rev. B **55**, 10613 (1997).
[28] Bing Dong, H. L. Cui, and X. L. Lei, Phys. Rev. B **69**, 035324 (2003).
[29] G. Schmidt, G. Richter, P. Grabs, C. Gould, D. Ferrand, and L. W. Molenkamp, Phys. Rev. Lett. **87**, 227203 (2001).
[30] W. Rudzinski and J. Barnas, Phys. Rev. B **64**, 085318 (2001).
[31] J. Martinek, J. Barnas, A. Fert, S. Maekawa, and G. Schn, J. Appl. Phys. **93**, 8265 (2003).
[32] A. Slobodskyy, C. Gould, T. Slobodskyy, C. R. Becker, G. Schmidt, and L. W. Molenkamp, Phys. Rev. Lett. **90**, 246601 (2003).
[33] A. Kogan, S. Amasha, D. Goldhaber-Gordon, G. Granger, M. A. Kastner, and H. Shtrikman, Phys. Rev. Lett. **93**, 166602 (2004).